Electronic Supplementary Material (ESI) for RSC Advances.


Electronic Supplementary Information (ESI) for:

# Metal ion size profoundly affects $H_3$glyox chelate chemistry

*Neha Choudhary,[a,b] Kendall E. Barett,[c] Manja Kubeil,[d] Valery Radchenko,[b,e] Jonathan Engle,[c] Holger Stephan,[d] María de Guadalupe Jaraquemada-Peláez*[a] and Chris Orvig*[a]*

[a] Medicinal Inorganic Chemistry Group, Department of Chemistry, University of British Columbia, 2036 Main Mall, Vancouver, British Columbia V6T 1Z1, Canada

[b] Life Sciences Division, TRIUMF, 4004 Wesbrook Mall, Vancouver, British Columbia V6T 2A3, Canada

[c] University of Wisconsin Department of Medical Physics, 1111 Highland Avenue, Madison, WI, 53711, USA

[d] Institute of Radiopharmaceutical Cancer Research, Helmholtz-Zentrum Dresden-Rossendorf, Bautzner Landstraße 400, D-01328 Dresden, Germany

[e] Department of Chemistry, University of British Columbia, 2036 Main Mall, Vancouver, British Columbia V6T 1Z1, Canada

*Corresponding Authors: Chris Orvig (orvig@chem.ubc.ca) and María de Guadalupe Jaraquemada-Peláez (mdgjara@chem.ubc.ca)

## Table of Contents

**NMR spectra of compounds 1-4**

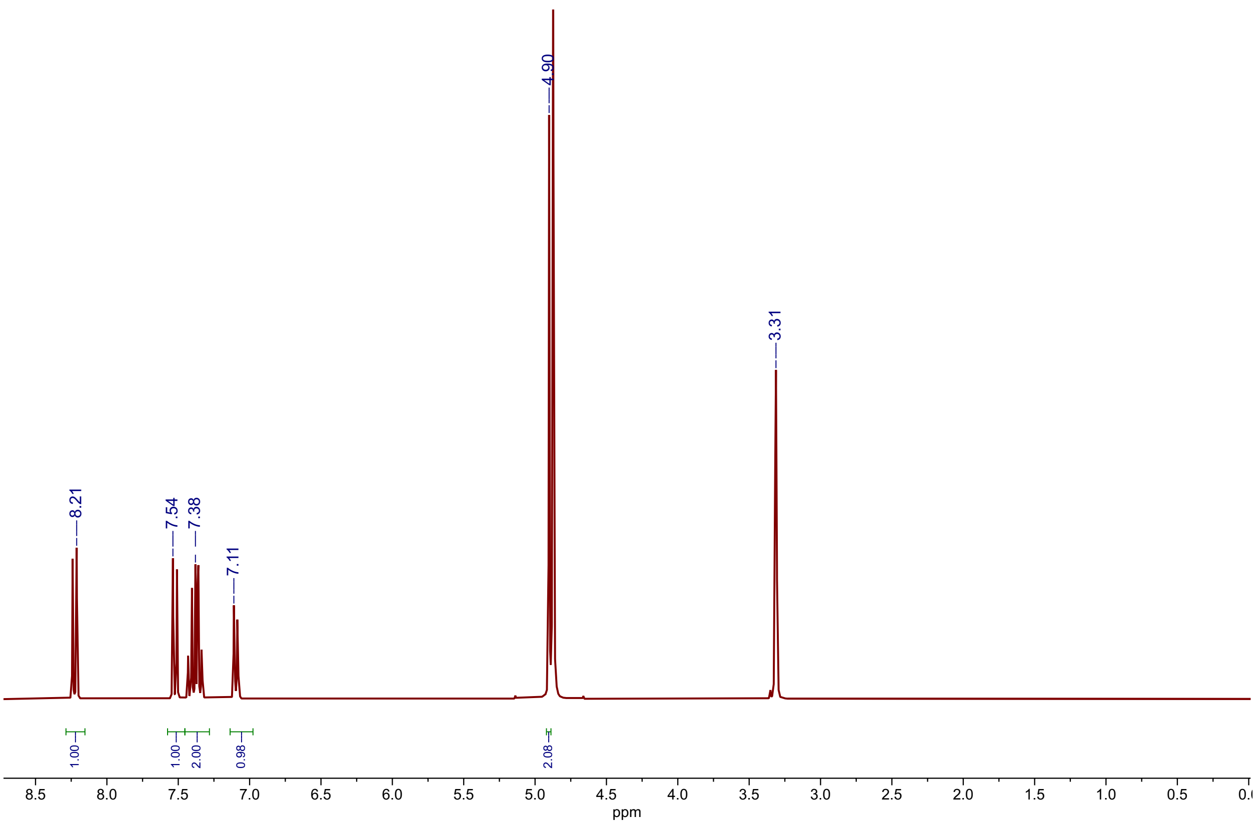


**Figure S1.** Compound **1** $^{1}H$ NMR spectrum (400 MHz, 298 K, MeOD-$d^4$).

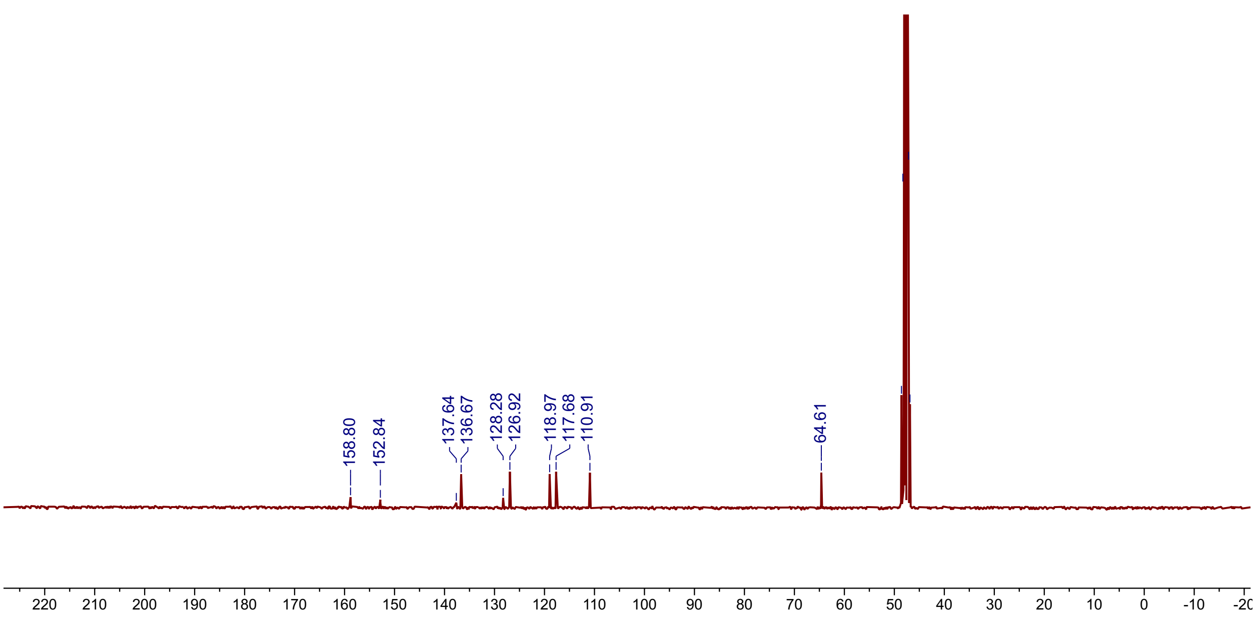


**Figure S2.** Compound **1** $^{13}C$ NMR spectrum (75 MHz, 298 K, MeOD-$d^4$).

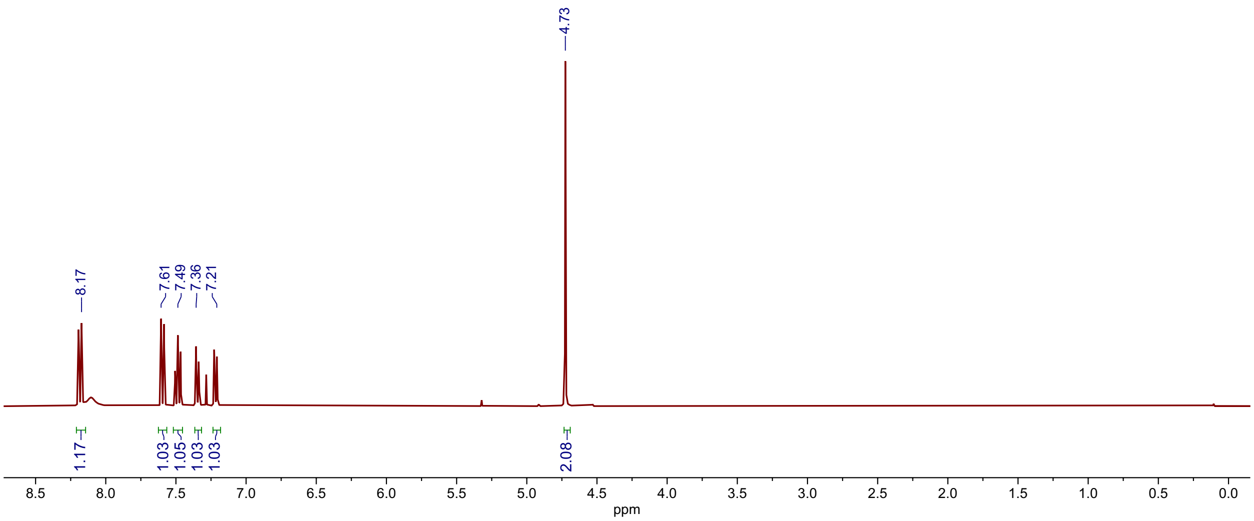


**Figure S3.** Compound **2** $^{1}H$ NMR spectrum (400 MHz, 298 K, $CDCl_3$).

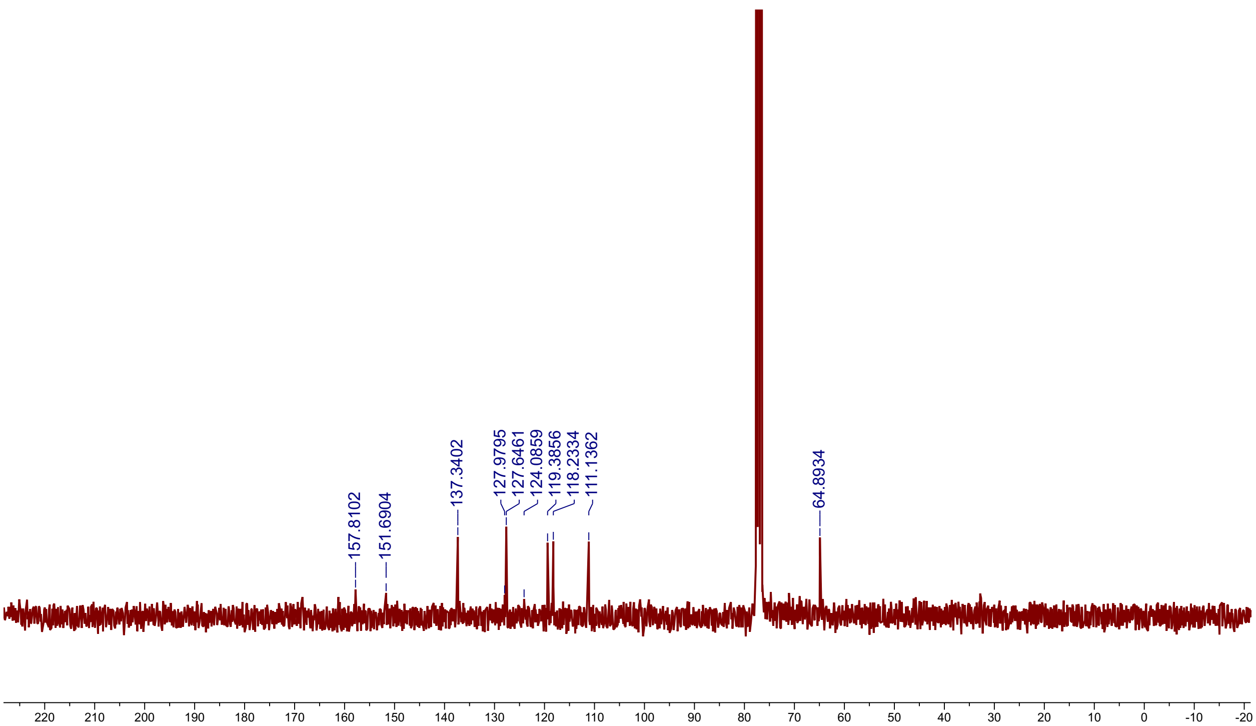


**Figure S4.** Compound **2** $^{13}C$ NMR spectrum (75 MHz, 298 K, $CDCl_3$).

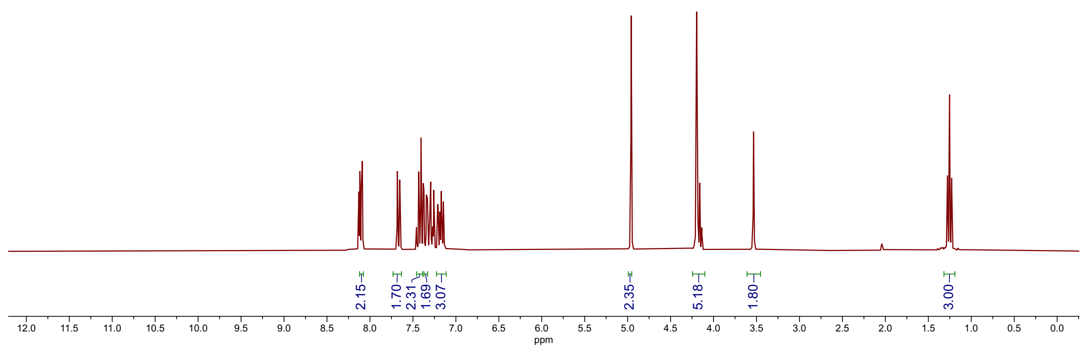


**Figure S5.** Compound **3** $^{1}H$ NMR spectrum (400 MHz, 298 K, $CDCl_3$).

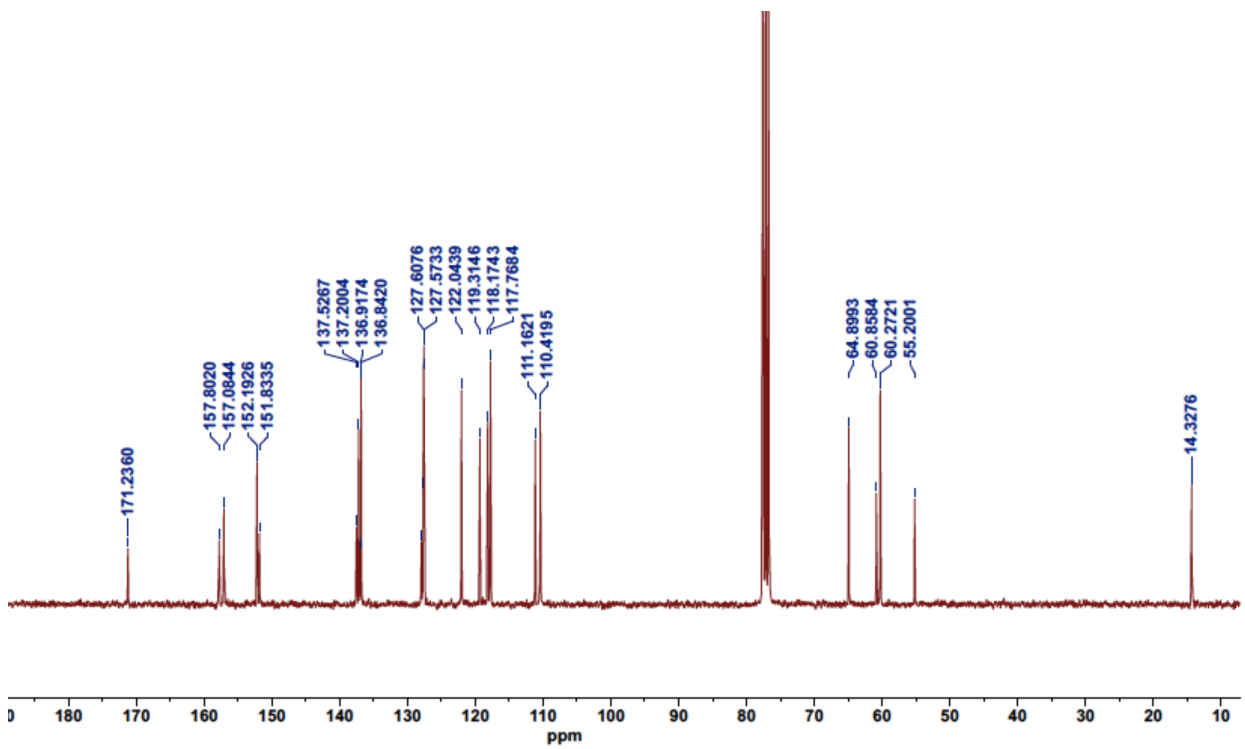


**Figure S6.** Compound **3** $^{13}C$ NMR spectrum (75 MHz, 298 K, $CDCl_3$).

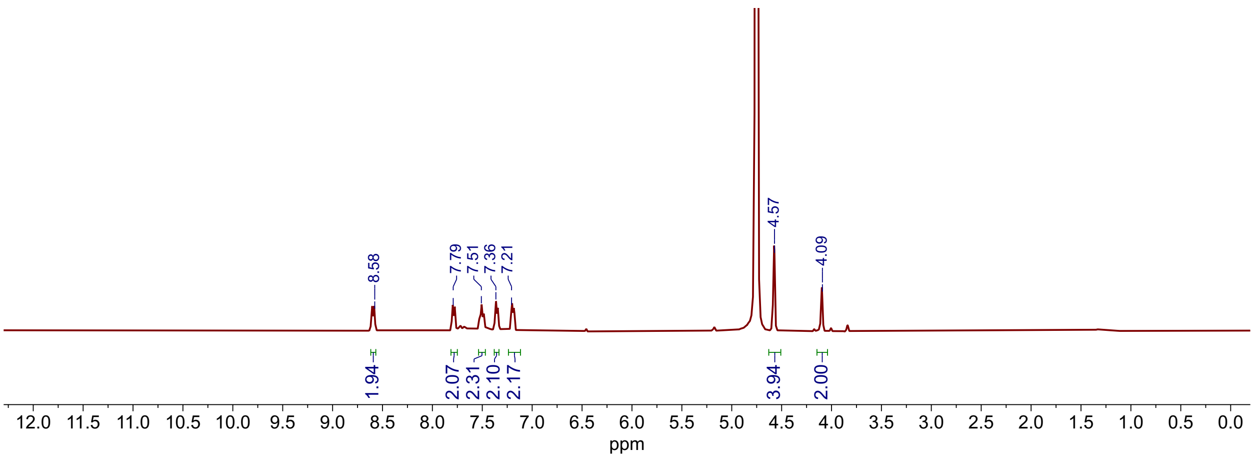


**Figure S7.** Compound **4,** $H_3$glyox $^1$H NMR spectrum (400 MHz, 298 K, $D_2O$).

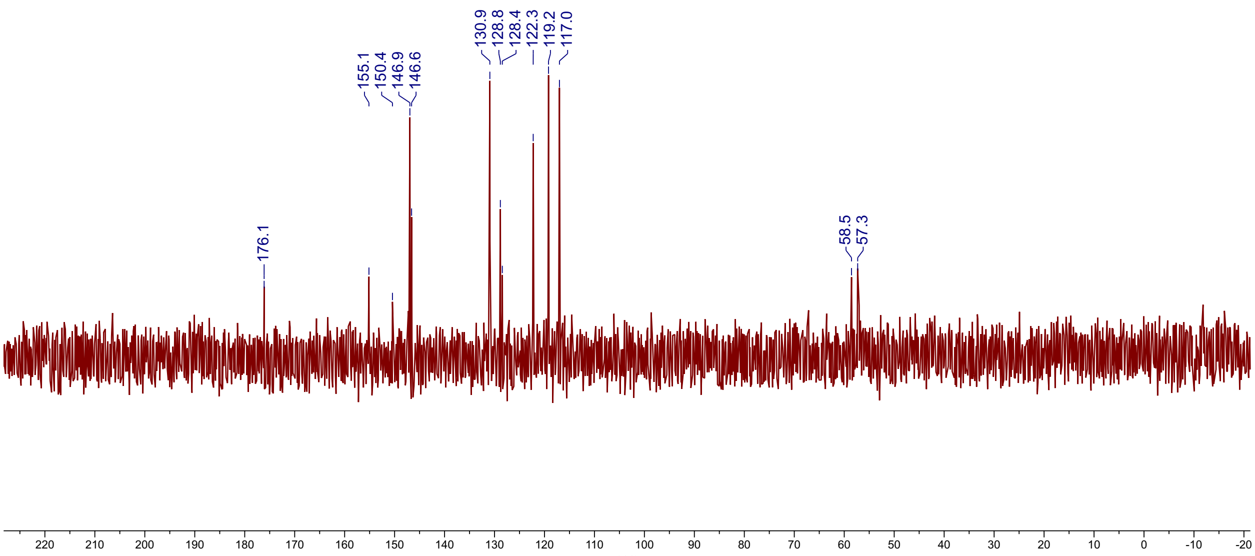


**Figure S8.** Compound **4** $^{13}$C NMR spectrum (75 MHz, 298 K, $D_2O$).

**Table S1.** High resolution mass spectra[a]

| **Species** | **Calculated Mass** | **Measured Mass** |
|---|---|---|
| $C_{22}H_{19}N_3O_4$ | 389.1400 | 390.1451 $[M + H]^+$ |
| $C_{22}H_{16}{}^{175}LuN_3O_4$ | 561.0548 | 562.0546 $[M + H]^+$ |
| $C_{22}H_{17}{}^{55}MnN_3O_4$ | 442.0599 | 443.0601 $[M + H]^+$ |
| $C_{22}H_{17}{}^{63}CuN_3O_4$ | 450.0515 | 473.0412 $[M + Na]^+$ |

[a] All masses obtained *via* high resolution electrospray ionization, positive mode.

## Solution thermodynamics

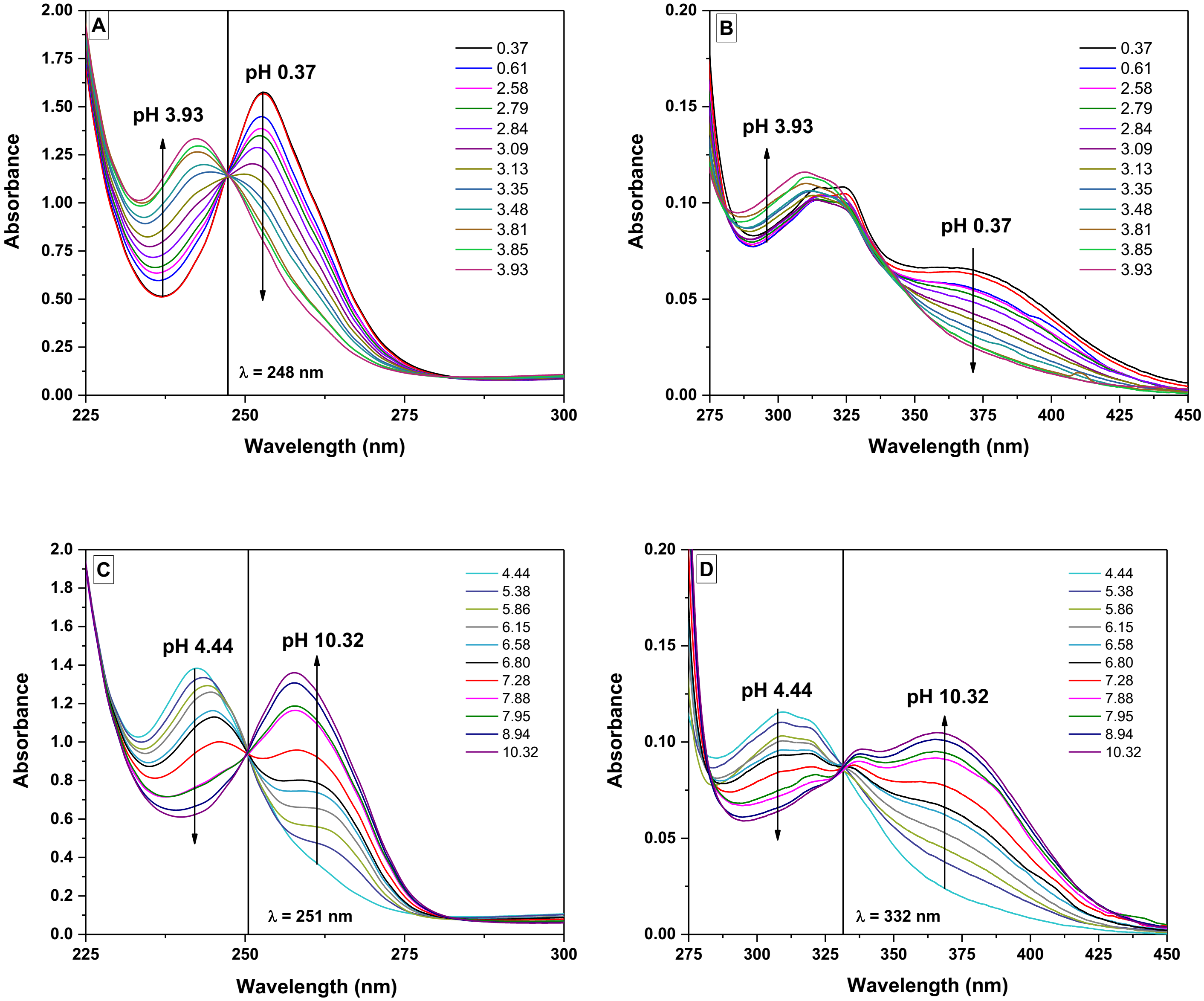


**Figure S9. (A-D)** Representative spectra of the in-batch UV spectrophotometric titration of $Mn^{2+}$-$H_3$glyox system [$H_3$glyox] = [$Mn^{2+}$] = 2.5 × $10^{-5}$ M at 25 °C, $I$ = 0.16 M (NaCl), l = 1 cm.

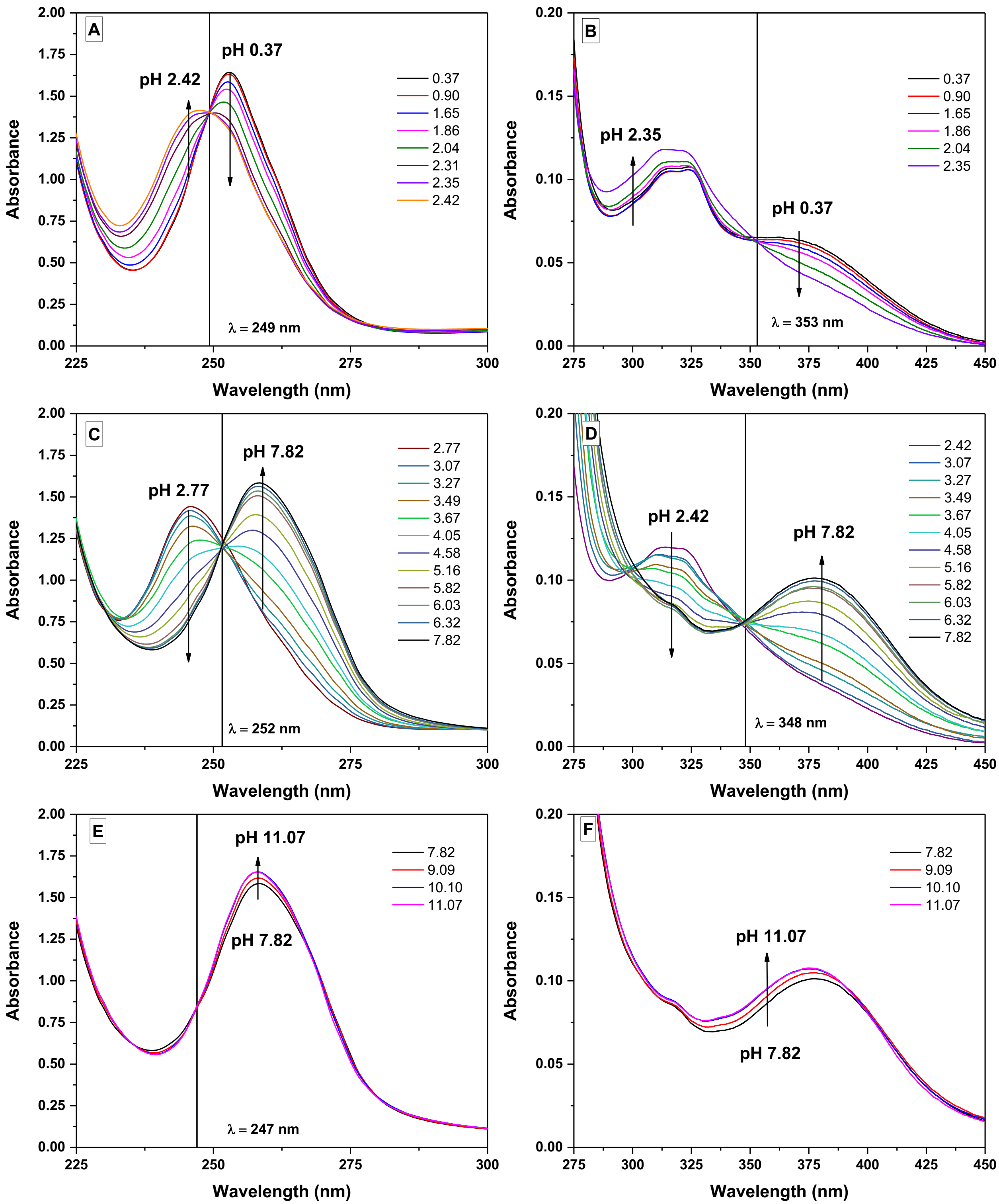


**Figure S10.** Representative spectra of the in-batch UV spectrophotometric titration of $Cu^{2+}$-$H_3$glyox system [$H_3$glyox] = [$Cu^{2+}$] = 2.5 × $10^{-5}$ M at 25 °C, $I$ = 0.16 M (NaCl), l = 1 cm.

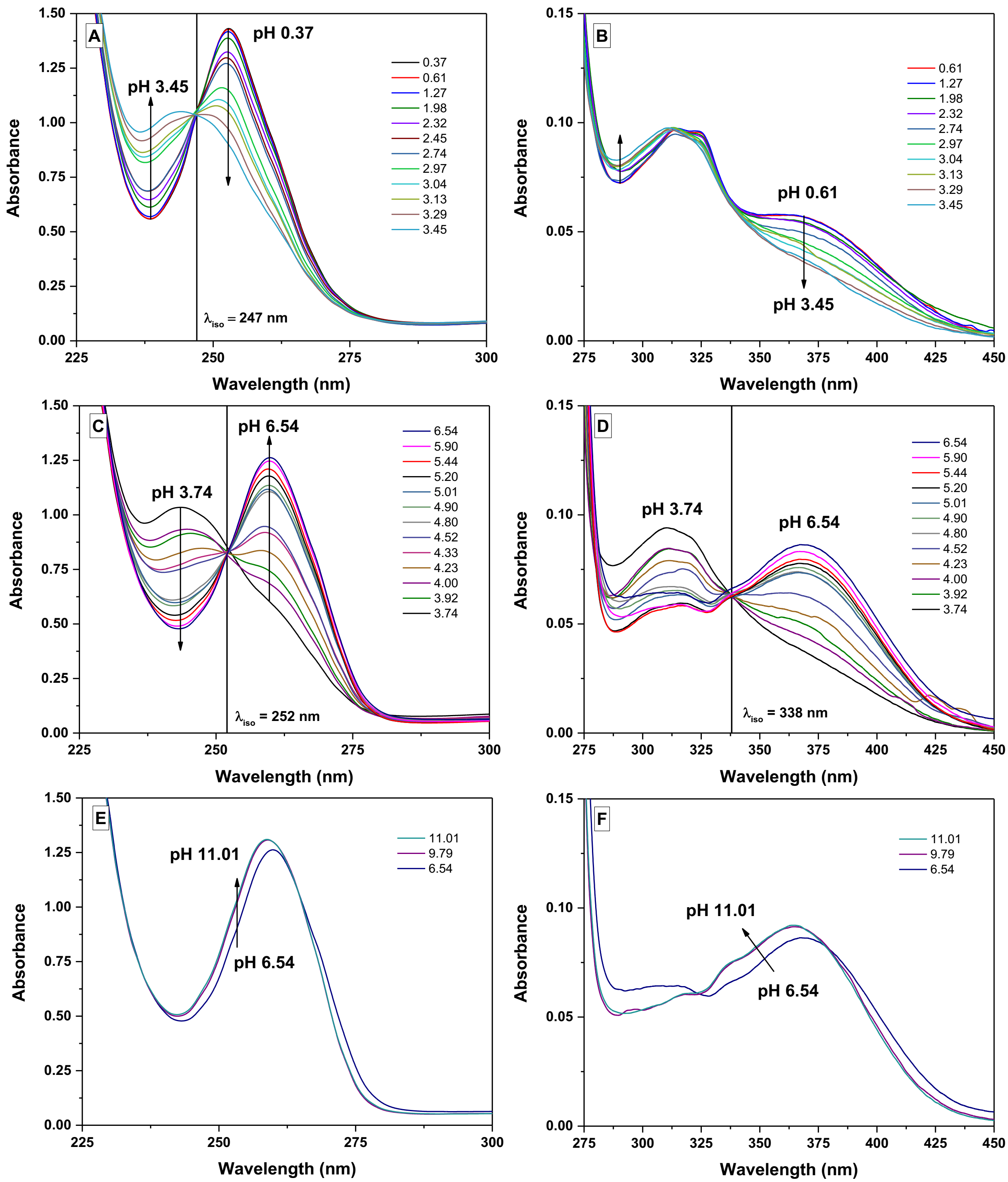


**Figure S11.** Representative spectra of the in-batch UV spectrophotometric titration of $Lu^{3+}$-$H_3$glyox system [$H_3$glyox] = [$Lu^{3+}$] = 2.17 × $10^{-5}$ M at 25 °C, $I$ = 0.16 M (NaCl), l = 1 cm.

## Radiolabeling

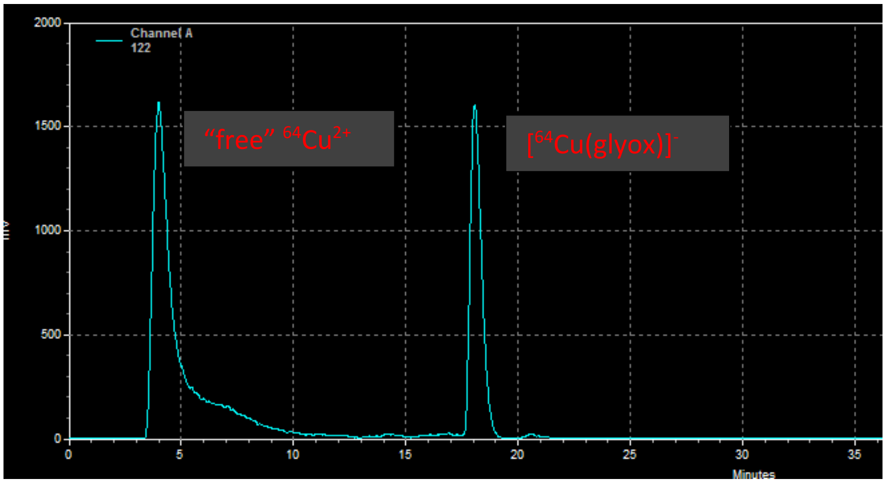


**Figure S12.** Radio-HPLC trace of free $[^{64}Cu]CuCl_2$ ($t_R$ = 4.0 min) and $[^{64}Cu][Cu(glyox)]^-$ ($t_R$ = 17.5 min) radiolabeled in 0.1 M NaOAc buffer pH 6, 15 min, RT, $[H_3glyox] = 10^{-4}$ M.

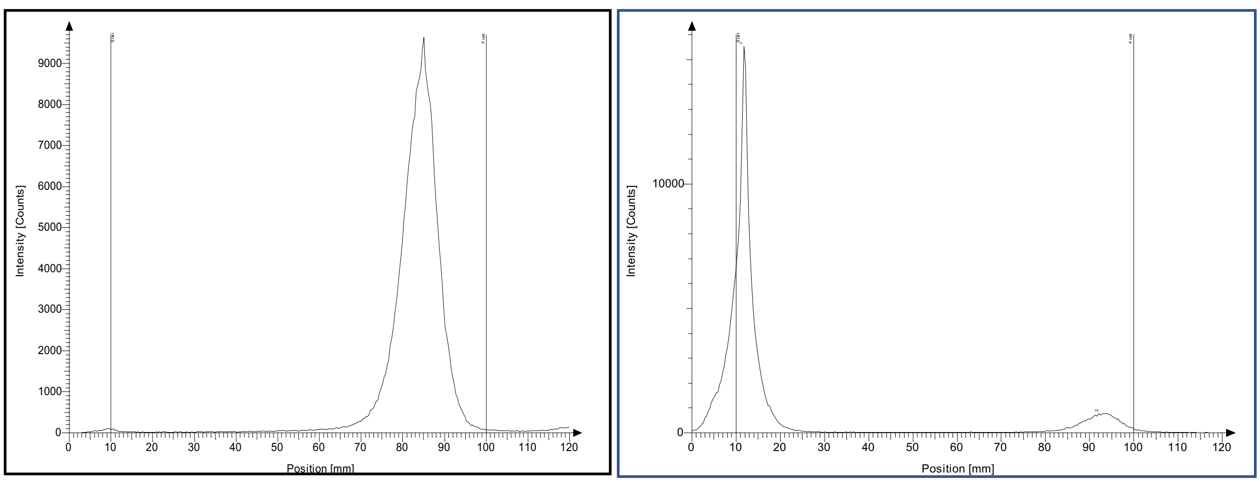


**Figure S13.** Crude i-TLC radiochromatographs of "free" $[^{64}Cu]Cu^{2+}$ (left) and $[^{64}Cu][Cu(glyox)]^-$ (right); stationary phase: gel silica plates, mobile phase: 0.1 M aq. EDTA solution pH 5.

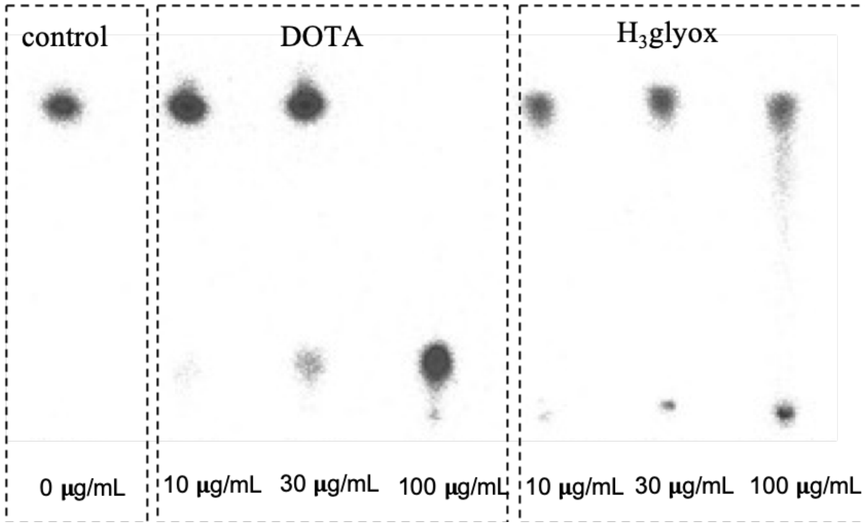


**Figure S14.** Crude i-TLC radiochromatographs of "free" [$^{52g}$Mn]$Mn^{2+}$, [$^{52g}$Mn]$Mn^{2+}$-DOTA complex and [$^{52g}$Mn]$Mn^{2+}$-$H_3$glyox with varying concentrations of DOTA and $H_3$glyox (Stationary phase: gel silica plates, mobile phase: 0.1 M aq. sodium citrate pH 5.5).

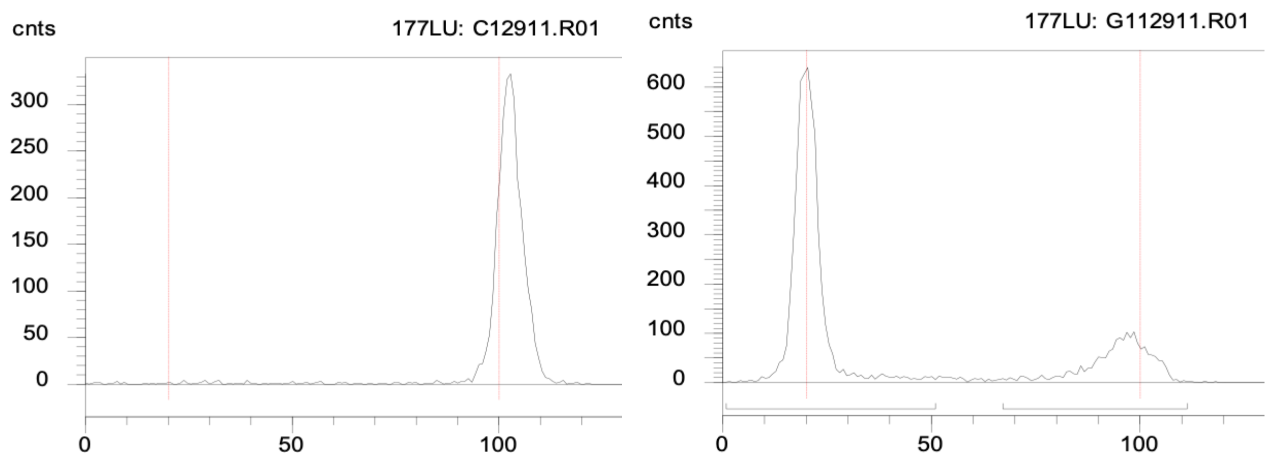


**Figure S15.** Crude i-TLC radiochromatographs of "free" [$^{177}$Lu]$Lu^{3+}$ (left) and [$^{177}$Lu]Lu(glyox) (right); stationary phase: gel silica plates, mobile phase: 0.1 M aq. EDTA solution pH 7.

## Density functional theory calculations

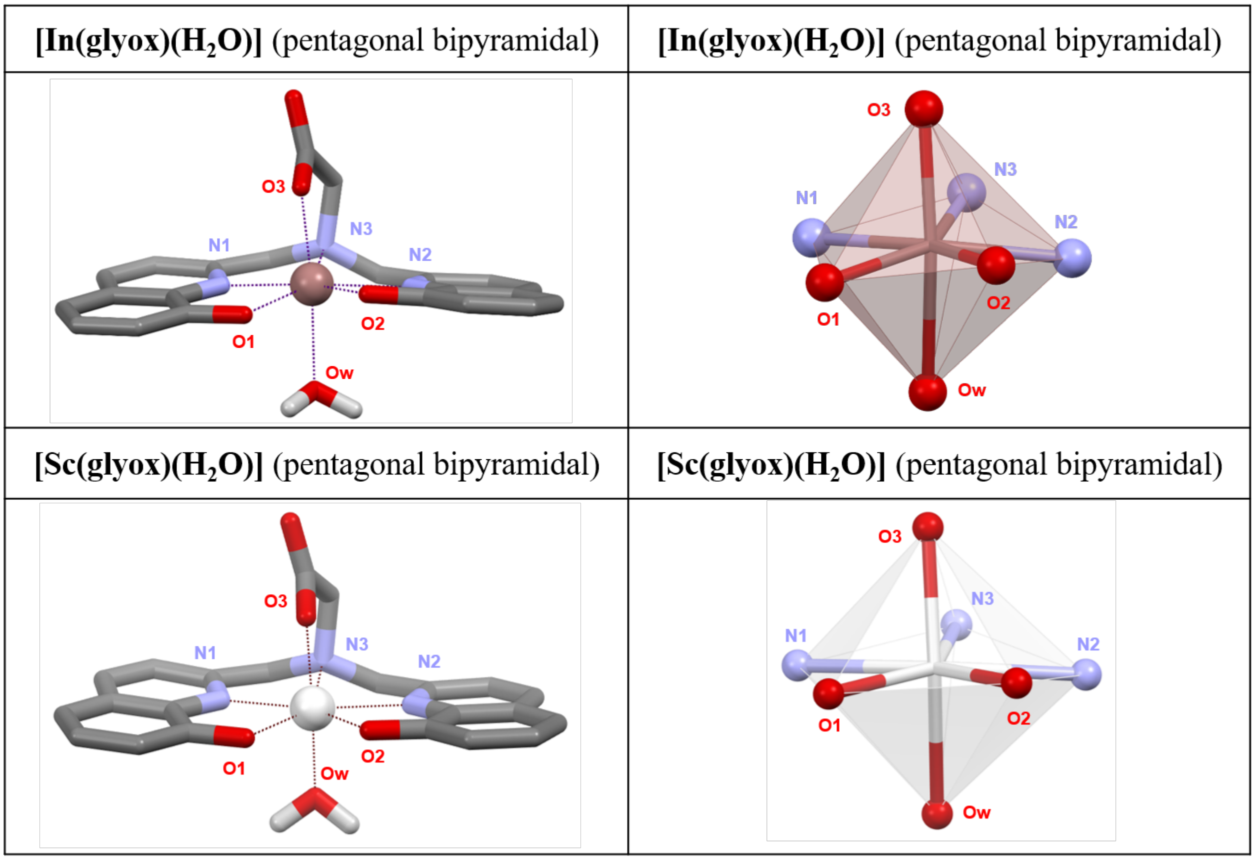


**Figure S16.** DFT calculated [In(glyox)($H_2O$)] and [Sc(glyox)($H_2O$)] structures.

**Table S2**. Bond lengths from calculated [In(glyox)($H_2O$)] and [Sc(glyox)($H_2O$)] DFT structures compared to the crystal structures.

| | **M-O (ligand) distances (Å)** | | | | **M-N (Ligand) Distances (Å)** | | |
|---|---|---|---|---|---|---|---|
| | COOH<br>**O3** | Ox 1<br>**O1** | Ox 2<br>**O2** | $H_2O$<br>**Ow** | Ox 1<br>**N1** | Ox 2<br>**N2** | 3° N<br>**N3** |
| **[In(glyox)($H_2O$)]** | 2.144 | 2.173 | 2.171 | 2.372 | 2.295 | 2.291 | 2.575 |
| **[In(glyox)($H_2O$)] crystal structure** | 2.179(3) | 2.175(5) | 2.163(6) | 2.186(8) | 2.269(6) | 2.265(6) | 2.546(4) |
| **[Sc(glyox)($H_2O$)]** | 2.040 | 2.085 | 2.085 | 2.259 | 2.314 | 2.314 | 2.555 |
| **[Sc(glyox)($H_2O$)] crystal structure** | 2.090(3) | 2.123(18) | 2.123(18) | 2.124(3) | 2.285(2) | 2.285(2) | 2.515(3) |

| $[Cu(glyox)(H_2O)]^-$ (square pyramidal) | $[Cu(glyox)(H_2O)]^-$ (square pyramidal) |
|---|---|
| 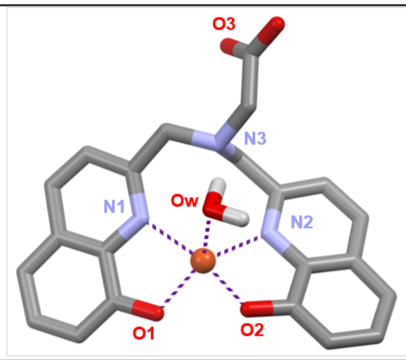  | 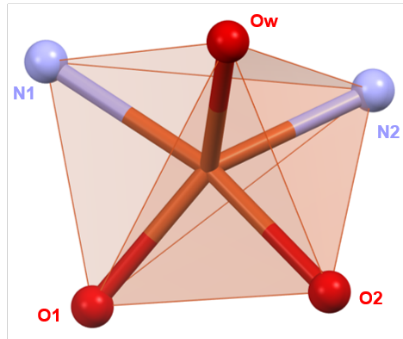  |
| $[Cu(glyox)]^- \cdot H_2O$ (square pyramidal) | $[Cu(glyox)]^- \cdot H_2O$ (square pyramidal) |
| 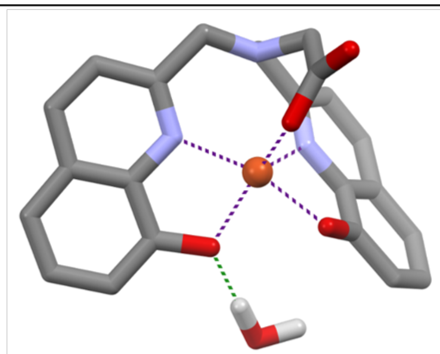 | 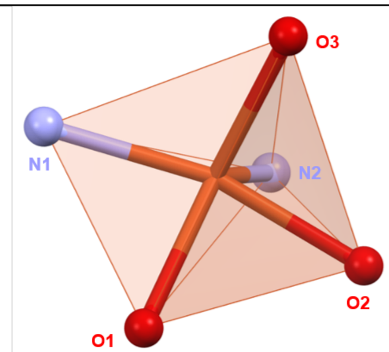  |

**Figure S17.** DFT calculated $[Cu(glyox)(H_2O)]^-$ and $[Cu(glyox)]^- \cdot H_2O$ structures.

**Table S3**. Bond lengths from calculated $[Cu(glyox)(H_2O)]^-$ and $[Cu(glyox)]^- \cdot H_2O$ structures.

| | **M-O (ligand) distances (Å)** | | | | **M-N (Ligand) Distances (Å)** | | | |
|---|---|---|---|---|---|---|---|---|
| | COOH **O3** | Ox 1 **O1** | Ox 2 **O2** | $H_2O$ **Ow** | Ox 1 **N1** | Ox 2 **N2** | 3° N **N3** | **Free E (Ha)** |
| **$[Cu(glyox)]^- \cdot H_2O$** | 2.048 | 2.015 | 2.011 | - | 2.072 | 2.205 | 2.765 | -1587.360 |
| **$[Cu(glyox)(H_2O)]^-$** | - | 1.930 | 1.962 | 2.357 | 2.136 | 2.086 | 3.234 | -1587.347 |
| | | | | | | | | |

**$[Cu(glyox)]^{-}\cdot 3H_2O$** (square pyramidal)

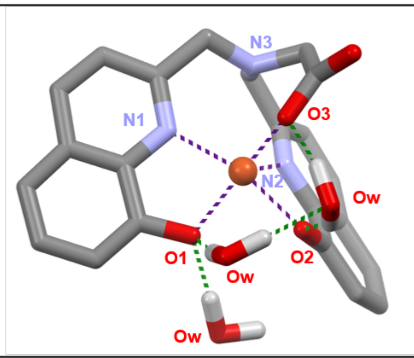


**$[Cu(glyox)]^{-}\cdot 3H_2O$** (square pyramidal)

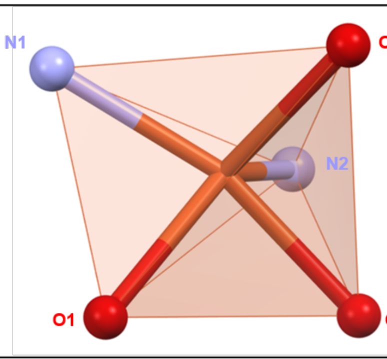


**$[Cu(glyox)(H_2O)]^{-}\cdot 2H_2O$** (square pyramidal)

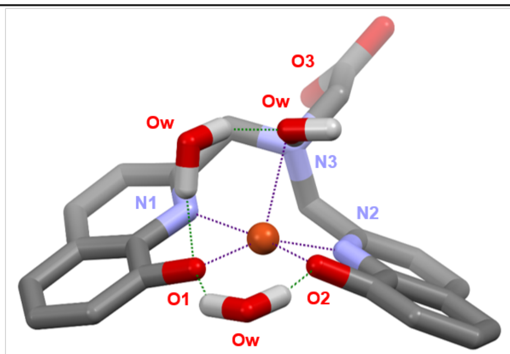


**$[Cu(glyox)(H_2O)]^{-}\cdot 2H_2O$** (square pyramidal)

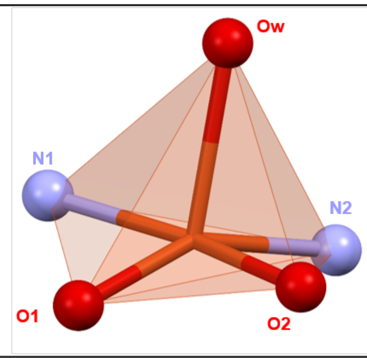


**Figure S18.** DFT calculated $[Cu(glyox)]^{-}\cdot 3H_2O$ and $[Cu(glyox)(H_2O)]^{-}\cdot 2H_2O$ structures.

**Table S4**. Bond lengths from calculated $[Cu(glyox)]^{-}\cdot 3H_2O$, $[Cu(glyox)(H_2O)]^{-}\cdot 2H_2O$ structures.

| | **M-O (ligand) distances (Å)** | | | | **M-N (Ligand) Distances (Å)** | | | |
|---|---|---|---|---|---|---|---|---|
| | COOH<br>**O3** | Ox 1<br>**O1** | Ox 2<br>**O2** | $H_2O$<br>**Ow** | Ox 1<br>**N1** | Ox 2<br>**N2** | 3° N<br>**N3** | **Free E (Ha)** |
| **$[Cu(glyox)]^{-}\cdot 3H_2O$** | 2.115 | 2.026 | 2.009 | - | 2.065 | 2.182 | 2.746 | -1740.268 |
| **$[Cu(glyox)(H_2O)]^{-}\cdot 2H_2O$** | - | 1.947 | 1.966 | 2.404 | 2.149 | 2.070 | 3.239 | -1740.252 |

**Table S5**. Bond lengths from calculated [Ga(glyox)($H_2O$)], [Mn(glyox)($H_2O$)]$^-$ and [Cu(glyox)]$^-$ DFT structures.

| | M-O (ligand) distances (Å) | | | | M-N (Ligand) Distances (Å) | | |
|---|---|---|---|---|---|---|---|
| | COOH | Ox 1 | Ox 2 | $H_2O$ | Ox 1 | Ox 2 | 3° N |
| | **O3** | **O1** | **O2** | **Ow** | **N1** | **N2** | **N3** |
| **[Ga(glyox)($H_2O$)]** | 1.933 | 2.002 | 1.999 | 2.191 | 2.245 | 2.233 | 2.644 |
| **[Mn(glyox)($H_2O$)]$^-$** | 2.066 | 2.065 | 2.069 | 2.325 | 2.149 | 2.211 | 2.764 |
| **[Cu(glyox)]$^-$** | 2.056 | 2.000 | 2.013 | - | 2.074 | 2.209 | 2.781 |

**Table S6**. Bond lengths from calculated [Lu(glyox)($H_2O$)$_2$]A, [Lu(glyox)($H_2O$)$_2$]B structures.

| | M-O (ligand) distances (Å) | | | | M-N (Ligand) Distances (Å) | | | |
|---|---|---|---|---|---|---|---|---|
| | COOH | Ox 1 | Ox 2 | $H_2O$ | Ox 1 | Ox 2 | 3° N | |
| | **O3** | **O1** | **O2** | **Ow** | **N1** | **N2** | **N3** | **Free E (Ha)** |
| **[Lu(glyox)($H_2O$)$_2$]A** | 2.252 | 2.238 | 2.275 | 2.400<br>2.481 | 2.439 | 2.423 | 2.600 | -2702.724 |
| **[Lu(glyox)($H_2O$)$_2$]B** | 2.230 | 2.282 | 2.207 | 2.467<br>2.407 | 2.448 | 2.439 | 2.649 | -2702.726 |

**Table S7.** Protonation constants (log $K_{HqL}$), stability constants (log $K_{ML}$), corresponding stepwise protonation constants (log $K_{1q1}$($MH_qL$)$^a$ and pM values of relevant $Mn^{2+}$ chelators.

| | **$H_3$glyox**[b] | **$H_3$dpaa**[c] | **PyC3A**[d] | **PCTA**[e] | **PC2A-EA**[e] |
|---|---|---|---|---|---|
| log $K_{HL}$ | 10.66(1) | 7.26(2) | 10.16(2) | 9.97 | 11.34(1) |
| log $K_{H2L}$ | 9.7(1) | 3.90(3) | 6.39(4) | 6.73 | 8.93(2) |
| log $K_{H3L}$ | 7.51(2) | 3.29(2) | 3.13(3) | 3.22 | 6.91(3) |
| log $K_{H4L}$ | 5.41(1) | 1.77(2) | - | 1.40 | 1.97(3) |
| log $K_{H5L}$ | 3.33(1) | - | - | - | - |
| log $K_{H6L}$ | 2.66(1) | - | - | - | - |
| **Σ log $K_{HqL}$** | **39.27** | **16.22** | **19.68** | **21.32** | **29.15** |
| log $K_{MnL}$ | 16.75(1) | 13.19(5) | 14.14(1) | 16.83 | 19.01(4) |
| log $K_{MnHL}$ | 7.17(1) | 2.90(6) | 2.43(3) | 1.96 | 6.88(2) |
| log $K_{MnH2L}$ | - | | - | - | 2.50(3) |
| log $K_{Mn(OH)L}$ | 10.45(2) | 11.97(6) | - | - | - |

$^a$ $K_{1q1}$ = [$MH_qL$]/[$MH_{q-1}L$][H]$^q$; [b]from ref.[1] [c]from ref.[4]; [d]from ref.[2]; [e]from ref.[3];

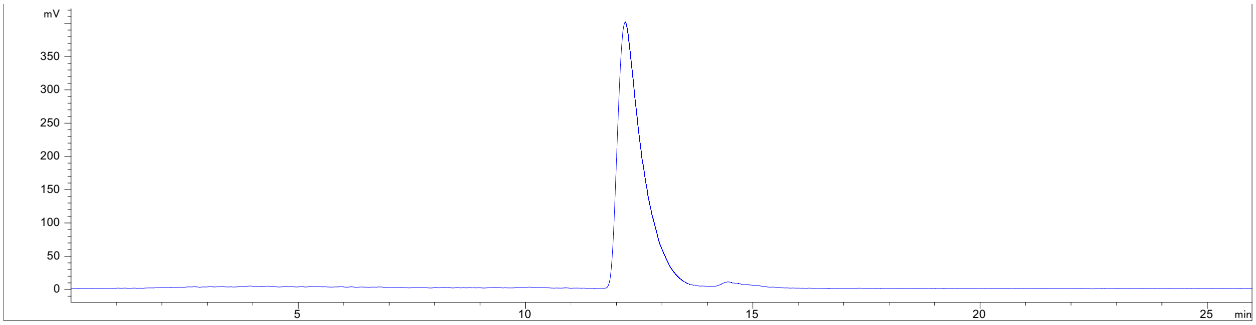


**Figure S19.** HPLC trace of H$_3$glyox ($t_R$ = 12.1 min); eluents: (A) 0.1% TFA in $H_2O$ and (B) 0.1% TFA in ACN with a linear gradient 5% to 100% B for 25 min and flow rate set to 1 mL/min..

## References

1 N. Choudhary, M. de G. Jaraquemada-Peláez, K. Zarschler, X. Wang, V. Radchenko, M. Kubeil, H. Stephan, C. Orvig, *Inorg. Chem.*, 2020, **59**, 5728–5741.

2 E. M. Gale, I. P. Atanasova, F. Blasi, I. Ay and P. Caravan, *J. Am. Chem. Soc.*, 2015, **137**, 15548–15557.

3 R. Botár, E. Molnár, G. Trencsényi, J. Kiss, F. K. Kálmán and G. Tircsó, *J. Am. Chem. Soc.*, 2020, **142**, 1662–1666.

4 A. Forgács, R. Pujales-Paradela, M. Regueiro-Figueroa, L. Valencia, D. Esteban-Gómez, M. Botta and C. Platas-Iglesias, *Dalton Trans.*, 2017, **46**, 1546–1558.